Charge-Density Waves Observed with a Tunneling Microscope

R. V. Coleman, B. Drake,[a] P. K. Hansma,[a] and G. Slough
Department of Physics, University of Virginia, Charlottesville, Virginia 22901
(Received 4 June 1985)

Charge-density waves on cleaved surfaces of $1T$-TaS_2 appeared at 77 K as hexagonal arrays of mounds with spacings of $(3.5 \pm 0.3)a_0$, where $a_0 = 3.346$ Å is the lattice spacing of the $1T$-TaS_2. In contrast, cleaved surfaces of $2H$-$TaSe_2$ at 77 K showed only atoms. The tunneling microscope was operated under liquid nitrogen with a $Pt_{0.8}Ir_{0.2}$ tip for both types of samples.

PACS numbers: 68.20.+t, 73.40.Gk

Tunneling microscopy is evolving into an important tool for surface analysis. Milestones in this evolution have included the profiling of grating surfaces,[1,2] observation of steps one atom high,[3-5] detailing of the atomic positions in semiconductor reconstructions,[6,7] demonstration of small-scale variations in the superconducting energy gap at the surface of a thin film,[8] observation of single atoms in a close-packed layer,[9] and spectroscopic imaging.[10] The above results were obtained with tunneling microscopes operating in vacuum.

Here we report the first results obtained with a tunneling microscope operating submerged in liquid nitrogen and show that charge-density waves (CDW's) can be observed directly. The liquid nitrogen was used to cool the sample below the charge-density wave transitions in layer-structure compounds and provided damping for mechanical vibrations.

The tunneling microscope was a hybrid between IBM Zurich designs[3-6] and squeezable electron tunneling junctions.[11-13] The x-y translator was cut from a $3 \times 3 \times 0.635$-cm^3 block of C5400 lead-titanate–lead-zirconate piezoelectric material.[14] The z translator was a half-circular bimorph made from two 1-mm-thick, 1.5-cm-radius half disks of C5800 lead-titanate–lead-zirconate piezoelectric material[14] glued together with epoxy. The z translator was supported about the x-y translator with three tungsten spacers near the edges and warped down in the center at ≈ 36 Å/V to bring the sample near the $Pt_{0.8}Ir_{0.2}$ tip.

The microscope was submerged in a Dewar of liquid nitrogen and supported by a spring. The Dewar was in turn supported by three rubber tubes from the ceiling. Details of the construction and operation of the microscope will be presented elsewhere.

Figure 1(a) shows individual atoms on a cleaved $2H$-$TaSe_2$ surface. It is a photograph of a storage oscilloscope screen. The horizontal deflection is 6.6 Å/division times the x motion across the sample. The vertical deflection is 6.6 Å/division times the y motion across the sample plus ≈ 18 Å/division times the z motion, giving a pseudo three-dimensional image. Crude calibrations were obtained by calculation based on the manufacturer's values for d_{31}, g_{31}, and ϵ_{33} followed by extrapolation to 77 K with use of another manufacturer's data[15] for similar materials.[16] A refined calibration for x and y motion, $\approx 20\%$ higher, was obtained by assuming that these were indeed atoms with the spacing given by Wilson and Yoffe[17]: 3.43 Å. This refined calibration was used for measuring the wavelength of the charge-density waves. A refined calibration for the z motion is not yet available.

Figure 1(b) shows charge-density waves on a cleaved surface of $1T$-TaS_2. A hexagonal array of

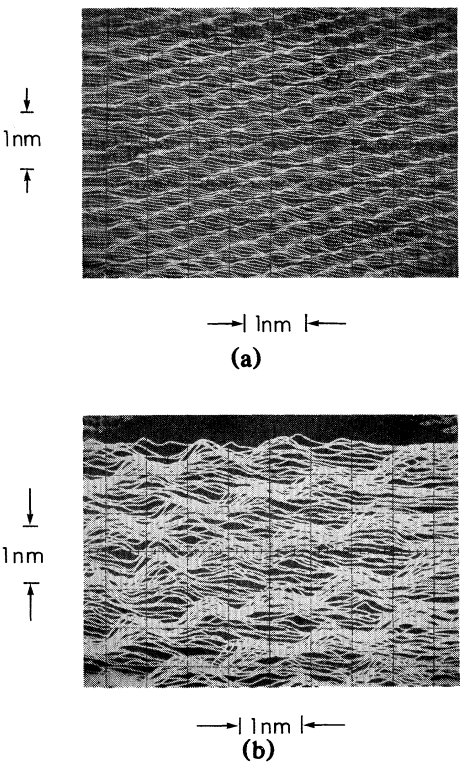

FIG. 1. (a) Atoms on a cleaved surface of $2H$-$TaSe_2$. The image was obtained in ≈ 5 sec at a scan rate of 10 Hz. The applied voltage was ≈ 50 meV and the tunneling current was 2 nA. (b) Charge-density waves on a cleaned surface of $1T$-TaS_2. The magnification and scan rate were the same as above. The applied voltage was ≈ 50 meV and the tunneling current was 5.5 nA.

mounds is clearly visible with a lattice spacing $\lambda_{CDW} = (3.5 \pm 0.3) a_0$, where $a_0 = 3.346$ Å.[17] The apparent height of the mounds is of order 4 Å, in contrast to of order 0.5 Å for the atoms in $2H$-$TaSe_2$ (although, as mentioned above, the calibration of the z axis is only approximate).

Photographs were taken with different scan rates and at different magnifications. At higher scan rates, > 15 Hz, the amplitude of the bumps was reduced. At lower scan rates, < 5 Hz, its overall shape was the same but random noise and drift were more troublesome. Thus we obtained the best results at the fastest scan rates at which the tip could track the surface, ≈ 10 Hz. Photographs at different magnifications were taken; the ones selected for this paper were a compromise to allow seeing of the atoms and the charge-density waves at the same magnification. In all, approximately thirty photographs of atoms on three different samples of $2H$-$TaSe_2$ and twenty photographs of charge-density waves on three different samples of $1T$-TaS_2 have been obtained. No clear photographs of atoms on $1T$-TaS_2 or charge-density waves on $2H$-$TaSe_2$ have been obtained.

$1T$-TaS_2 and $2H$-$TaSe_2$ both show superlattices due to charge-density wave formation and at 77 K the CDW's are commensurate in both crystals. In $1T$-TaS_2 the CDW forms at high temperatures (~ 600 K) oriented along three equivalent a-axis directions with $\lambda_{CDW} = 3.6 a_0$.[18,19] This gives a triple CDW lattice which is incommensurate with the crystal lattice. At 350 K there is a first-order transition where the triple CDW rotates to approximately 11° away from the a axis in an attempt to become commensurate. Finally, near 200 K another first-order transition occurs in which the triple CDW becomes commensurate with a rotation of 13.9° from the a axis and $\lambda_{CDW} = \sqrt{13} a_0$. In the low-temperature commensurate phase, the unit cell is triclinic and contains thirteen formula units, so that the full superlattice is $\sqrt{13} a_0 \times \sqrt{13} a_0 \times 13 c_0$.

In[20] $2H$-$TaSe_2$ an incommensurate triple CDW forms in a second-order (or nearly second-order) transition at 122.3 K followed by a first-order transition near 90 K below which the CDW superlattice is commensurate with $\lambda_{CDW} = 3 a_0$. The superlattice is then $3 a_0 \times 3 a_0 \times c_0$ resulting from the superposition of three CDW's.

The formation of the CDW's is accompanined by a periodic structural distortion in which the atomic displacements are on the order of 0.1 to 0.25 Å. The CDW transitions are driven by Fermi-surface instabilities[21] with wave vectors near $2k_F$ and result in substantial gapping of the high-temperature Fermi surface. This can result in almost complete annihilation of the Fermi-surface area or in a substantial rearrangement of the Fermi-surface geometry.

In the case of $1T$-TaS_2 the gapping of the Fermi surface results in an extremely low carrier concentration in the commensurate state and at the lowest temperatures the resistivity rises indicating either semiconducting[22] behavior or some type of metal-insulator transition[23] (see Fig. 2). The band calculations of Myron and Freeman[24] showed that in the commensurate phase nesting occurred over substantial regions of the Fermi surface consistent with a large reduction of Fermi-surface area in the CDW phase. If an activated conductivity is assumed the activation energy derived from Arrhenius plots of $\rho_{\|}$ vs T between 50 and 150 K is $\Delta \approx 5$ meV although a single energy gap does not suffice at all temperatures. X-ray photoelectron spectroscopy[25] of the Ta $4f$ core levels also showed that the CDW amplitude in $1T$-TaS_2 was extremely large at low temperatures, on the order of one electron per atom. The CDW transitions in $1T$-TaS_2 produce large changes in the resistivity parallel to the layers as shown in Fig. 2. All of these observations suggest that a large fraction of the conduction electrons have condensed into the CDW phase at 77 K.

In contrast to $1T$-TaS_2 the $2H$-$TaSe_2$ resistivity parallel to the layers as also shown in Fig. 2 shows only a small anomaly at the CDW transition (120 K) and the

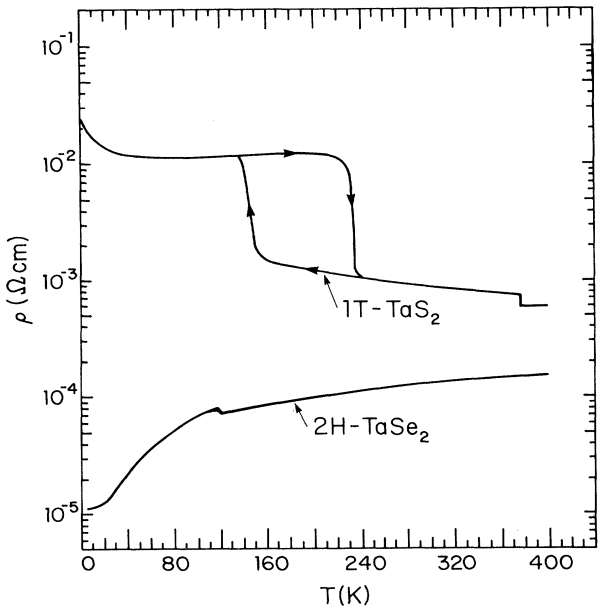

FIG. 2. The resistivity of $1T$-TaS_2 and $2H$-$TaSe_2$ measured parallel to the layers vs temperature. The resistivity of $1T$-TaS_2 shows much larger anomalies at the CDW phase changes than observed in $2H$-$TaSe_2$. $1T$-$TaSe_2$ shows a two-part incommensurate to commensurate transition with discontinuous resistance changes at 350 and 200 K with an initial CDW onset at ~ 600 K. $2H$-$TaSe_2$ has an initial CDW onset at 120 K with lock-in at 90 K and a very weak resistance anomaly.

resistivity remains metallic down to the lowest temperatures. The Fermi surface is gapped by the CDW, but this results in substantial rearrangement of the Fermi surface due to band folding rather than annihilation. A large number of normal electrons remain below the CDW transition. Wilson[26] in a band-folding model attempted to identify the parts of the $2H$-$TaSe_2$ Fermi surface affected by the CDW. Details of the CDW structure and phasing in $2H$-$TaSe_2$ have also been given by Wilson[27] and Wilson and Vincent.[28]

De Haas–van Alphen[29] and Shubnikov–de Haas[30] experiments on $2H$-$TaSe_2$ show up to eleven frequencies in the range 1 to 45 MG. The angular dependence of these frequencies can be fitted by undulating cylinders running parallel to the c axis consistent with the two-dimensional character of these layer-compound Fermi surfaces. Doran and Woolley[31] have presented detailed calculations of the band-structure density of states and total band-structure energy of the $2H$ phase in the 3×3 CDW state. They find six doubly degenerate electron cylinders and their calculated density of states is similar to that calculated for the normal high-temperature phase.[32] In both cases the Fermi energy lies just above the main peak suggesting that the peak is an important feature in the CDW stabilizing. Although the details of this peak vary with CDW amplitude the magnitude of the density of states at the Fermi level does not seem to vary substantially from that of the high-temperature phase.

The tunneling-microscopy results reported here clearly reflect the large differences in the CDW condensate that exist between $1T$-TaS_2 and $2H$-$TaSe_2$. The local tunneling density of states in the case of $1T$-TaS_2 appears to be dominated by the CDW condensate structure while in $2H$-$TaSe_2$ the presence of a large number of normal electrons below the CDW transition causes the local tunneling density of states to be predominately modulated at the lattice period of 3.43 Å.

A detailed microscopic model of how the CDW condensate contributes to the local tunneling density of states needs to be developed. The tunneling directions in these experiments are predominately perpendicular to the layers while the group velocities of the electrons are predominately parallel to the layers. This may introduce some directional anisotropy into the problem as well as the need to consider anisotropy in the CDW gap structure in any detailed analysis. Nevertheless the results have shown that the tunneling microscope is highly sensitive to the details of the charge-density-wave transition in representative layer compounds. In addition the ability to produce highly perfect surfaces by cleaving makes the transition-metal dichalcogenides ideal specimens for tunneling microscopy. The characteristic of layer structures has also been used to advantage in molecular-beam diffraction by Boato, Cantini, and Collella.[33] They used helium-beam diffraction to observe satellite peaks corresponding to the surface-corrugation effects due to charge-density waves in $1T$-TaS_2. Experiments are under way on a number of other phases and compounds which exhibit CDW transitions in order to further characterize the ability of tunneling microscopy to detect charge-density wave structure.

We are indebted to G. Binnig, S. Chiang, J. Clarke, S. Elrod, R. Feenstra, J. A. Golovchenko, R. Jaklevic, W. J. Kaiser, C. Quate, and H. Rohrer for sharing freely their experience in building tunneling microscopes. We thank V. Celli, I. P. Batra, N. Garcia, and P. Hanmann for helpful conversations on theory, S. Alexander, M. Cullen, J. Schneer, and R. Sonnenfeld for their practical advice, and W. McNairy for help with data analysis. This work was supported in part by the U. S. Office of Naval Research and U. S. Department of Energy Grant No. DE-FG05-85ER45072.

---

[a]On leave from Department of Physics, University of California, Santa Barbara, Cal. 93106.

[1]R. Young, Phys. Today **24**, No. 11, 42 (1971).

[2]R. Young, J. Ward, and F. Scire, Rev. Sci. Instrum. **47**, 1303 (1976).

[3]G. Binnig, H. Rohrer, Ch. Gerber, and E. Weibel, Phys. Rev. Lett. **49**, 57 (1982).

[4]G. Binnig and H. Rohrer, Surf. Sci. **126**, 236 (1983).

[5]G. K. Binnig, H. Rohrer, Ch. Gerber, and E. Stoll, Surf. Sci. **144**, 321 (1984).

[6]G. Binnig, H. Rohrer, Ch. Gerber, and E. Weibel, Phys. Rev. Lett. **50**, 120 (1983).

[7]J. A. Golovchenko, Bull. Am. Phys. Soc. **30**, 251 (1985).

[8]S. A. Elrod, A. L. de Lozanne, and C. R. Quate, Appl. Phys. Lett. **45**, 1240 (1984).

[9]C. Quate, Bull. Am. Phys. Soc. **30**, 251 (1985).

[10]G. Binnig, Bull. Am. Phys. Soc. **30**, 251 (1985).

[11]J. Moreland, S. Alexander, M. Cox, R. Sonnenfeld, and P. K. Hansma, Appl. Phys. Lett. **43**, 387 (1983).

[12]J. Moreland and P. K. Hansma, Rev. Sci. Instrum. **55**, 399 (1984).

[13]J. Moreland, J. Drucker, P. K. Hansma, J. P. Katthaus, A. Adams, and R. Kvaas, Appl. Phys. Lett. **45**, 104 (1984).

[14]Channel Industries, Santa Barbara, California.

[15]"Piezoelectric Technology Data for Designers" (Vernitron, Bedford, Ohio).

[16]C5400 is similar to PZT4; C5800 is similar to PZT8 according to M. Cullen of Channel Industries.

[17]J. A. Wilson and A. D. Yoffe, Adv. Phys. **18**, 193 (1969).

[18]J. A. Wilson and F. J. DiSalvo, and S. Mahajan, Adv. Phys. **24**, 117 (1975), and Phys. Rev. Lett. **32**, 882 (1974).

[19]C. B. Scruby, P. M. Williams, and G. S. Parry, Philos. Mag. **31**, 255 (1975).

[20]D. E. Moncton, J. D. Axe, and F. J. DiSalvo, Phys. Rev. Lett. **34**, 734 (1975).

[21]A. W. Overhauser, Phys. Rev. **167**, 691 (1968), and Phys. Rev. B **3**, 3173 (1971).
[22]J. P. Tidman and R. F. Frindt, Can. J. Phys. **54**, 2306 (1976).
[23]F. J. DiSalvo and J. E. Graebner, Solid State Commun. **23**, 825 (1977).
[24]H. W. Myron and A. J. Freeman, Phys. Rev. B **11**, 2735 (1975).
[25]G. K. Wertheim, F. J. DiSalvo, and S. Chiang, Phys. Rev. B **13**, 5476 (1976).
[26]J. A. Wilson, Phys. Rev. B **15**, 5746 (1977).
[27]J. A. Wilson, J. Phys. F **15**, 591 (1985).
[28]J. A. Wilson and R. Vincent, J. Phys. F **14**, 123 (1984).
[29]J. E. Graebner, Solid State Commun. **21**, 353 (1977).
[30]R. M. Fleming and R. V. Coleman, Phys. Rev. B **16**, 302 (1977).
[31]N. J. Doran and A. M. Woolley, J. Phys. C **14**, 4257 (1981).
[32]N. J. Doran and A. M. Woolley, *Physics of Semiconductors,* edited by B. L. H. Wilson, IOP Conference Proceedings No. 43 (Institute of Physics and the Physical Society, London, 1978), p. 911.
[33]G. Boato, P. Cantini, and R. Colella, Phys. Rev. Lett. **42**, 1635 (1979).

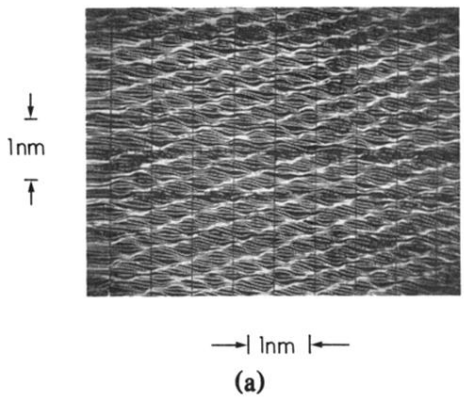

FIG. 1. (a) Atoms on a cleaved surface of $2H$-$TaSe_2$. The image was obtained in ≈ 5 sec at a scan rate of 10 Hz. The applied voltage was ≈ 50 meV and the tunneling current was 2 nA. (b) Charge-density waves on a cleaned surface of $1T$-TaS_2. The magnification and scan rate were the same as above. The applied voltage was ≈ 50 meV and the tunneling current was 5.5 nA.